ISSN 1807-1929
Revista Brasileira de Engenharia Agrícola e Ambiental
Brazilian Journal of Agricultural and Environmental Engineering
v.26, n.7, p.502-512, 2022
Campina Grande, PB – http://www.agriambi.com.br – http://www.scielo.br/rbeaa

DOI: http://dx.doi.org/10.1590/1807-1929/agriambi.v26n7p502-512

Foam mat drying kinetics of jambolan and acerola mixed pulp[1]

Cinética de secagem em camada de espuma da polpa mista de jambolão e acerola

Joana D'arc P. de Matos[2*], Rossana M. F. de Figueirêdo[2], Alexandre J. de M. Queiroz[2], Maria S. de Moraes[2], Semirames do N. Silva[2] & Luis P. F. R. da Silva[2]

[1] Research developed at Laboratory of Processing and Storage of Agricultural Products, Universidade Federal de Campina Grande, Campina Grande, PB, Brazil
[2] Universidade Federal de Campina Grande, Campina Grande, PB, Brazil

HIGHLIGHTS:

It was verified that the combination of foaming/stabilizing agents influenced the drying process.
Foam mat drying produced mixed pulp powders with low water content, important for their shelf life.
Effective diffusivity increases as a function of drying temperature elevation for jambolan and acerola mixed pulp.

ABSTRACT: Acerola and jambolan are fruits with several bioactive compounds of phenolic origin and a product made with these two raw materials appears to be a food with high antioxidant and nutraceutical potential. Therefore, this study aimed to evaluate the foam mat drying of the mixed pulp of jambolan and acerola. Mixed pulp formulations, containing 1.0% albumin with 0.5% xanthan gum (F1), 0.5% carboxymethylcellulose (F2) and 0.5% guar gum (F3), were dehydrated at 50, 60, 70 and 80 °C, with foam mat thickness of 0.5 cm. The elevation of the drying temperature decreased the water content and dehydration time of the samples. Formulation F3 obtained the shortest drying times; all drying models resulted in good adjustments, especially Midilli. Formulation F3 obtained greater effective diffusivity; the activation energy was higher in the F1 combination. The samples with albumin-guar (F3) showed greater enthalpy and entropy and samples with albumin-xanthan gum (F1) showed the highest Gibbs free energy. Foam mat drying is an efficient way of preserving the jambolan and acerola mixed pulp.

Key words: *Malpighia emarginata*, *Syzygium cumini*, dehydration, effective diffusivity, activation energy

RESUMO: A acerola e o jambolão são frutos com diversos compostos bioativos de origem fenólica e a composição de um produto elaborado com essas duas matérias-primas se afigura como um alimento com elevado potencial antioxidante e nutracêutico. Diante disso, este estudo foi realizado com o objetivo de avaliar a secagem em camada de espuma da polpa mista de jambolão e acerola. Foram elaboradas formulações com a polpa mista, contendo 1,0% de albumina com 0,5% de goma xantana (F1), 0,5% de carboximetilcelulose - CMC (F2) e 0,5% de goma guar (F3), desidratadas a 50, 60, 70 e 80 °C, com espessura da camada de espuma de 0,5 cm. A elevação da temperatura de secagem diminuiu o teor de água e tempo de desidratação das amostras. Os menores tempos de secagem foram obtidos na formulação F3; todos os modelos de secagem resultaram em bons ajustes, com destaque para Midilli. A maior difusividade efetiva foi obtida na formulação F3; a energia de ativação foi maior na combinação da F1. As amostras com albumina-guar (F3) apresentaram maiores entalpia e entropia e as com albumina-xantana (F1) as maiores energias livres de Gibbs. A secagem em camada de espuma é uma forma eficiente de conservação da polpa mista de jambolão e acerola.

Palavras-chave: *Malpighia emarginata*, *Syzygium cumini*, desidratação, difusividade efetiva, energia de ativação

• Ref. 250435 – Received 29 Mar, 2021
* Corresponding author - E-mail: joanadarcpma@hotmail.com
• Accepted 09 Feb, 2022 • Published 21 Feb, 2022
Editors: Josivanda Palmeira Gomes & Walter Esfrain Pereira

Introduction

Acerola (*Malpighia emarginata* D.C.) is a tropical fruit rich in vitamin C and phenolic compounds. Because of favorable soil and climate conditions, Brazil is a major producer of acerola in South America (Nogueira et al., 2019).

Syzygium cumini (L.) Skeels is a tree species with origins in tropical Asia (Seraglio et al., 2018). It produces jambolan or Java plum, with a predominance of sweet and astringent flavor, whose intensity is reduced with the advance of maturation. It contains several bioactive compounds, which are nutritionally important (Panghal et al., 2019).

Healthy eating has become an important consumer demand. In this scenario, fruits stand out for their high concentrations of vitamins, minerals and bioactive compounds. Fruits are susceptible to rapid post-harvest physiological deterioration. It is essential to subject them to processes that prolong their useful life, and one of the most promising alternatives available is drying (Chhikara et al., 2018; Moreira et al., 2018).

Foam mat drying is a process that involves the conversion of a liquid or semi-liquid material into stable foam through the addition of foaming agent and drying within the temperature range that varies from 50 to 80 °C. It has the advantage of shorter drying time and greater savings compared to other techniques (Tan & Sulaiman, 2019).

Mixed pulp of jambolan and acerola forms a combination with high nutritional potential, particularly because of bioactive compounds such as ascorbic acid and phenolic compounds and attractive flavor and color. Drying this mixed pulp results in a potentially interesting product for the agribusiness and the consumer. In this context, the objective of this study was to evaluate the effect of drying temperatures on the foam mat drying kinetics of the mixed pulp of jambolan and acerola and the hygroscopic behavior of the products obtained.

Material and Methods

The study was conducted at the Agricultural Products Storage and Processing Laboratory, belonging to the Agricultural Engineering Academic Unit, Federal University of Campina Grande (UFCG), Campina Grande campus, PB, Brazil.

The raw materials used in this process were the mature specimens of jambolan (*Syzygium cumini* (L.) Skeels) and acerola (*Malpighia emarginata* D.C.), from the municipality of Macaíba, State of Rio Grande do Norte, Brazil (latitude 5° 51' 36" S, longitude 35° 20' 59" W, and altitude of 15 m), and the additives albumin (Infinity Pharma®, Campinas, SP, Brazil); Sodium Carboxymethyl Cellulose (CMC - Neon®, Suzano, SP, Brazil); guar gum (GastronomyLab®, Brasília, DF, Brazil) and xanthan gum (GastronomyLab®, Brasília, DF, Brazil).

Ripe fruits were selected based on skin color, when they showed red skin color in the acerola and dark purple skin color in the jambolan. The fruits were washed in running water and sanitized by immersion in 50 mg L^{-1} sodium hypochlorite solution for 15 min. Subsequently, they were rinsed and passed through a horizontal pulper (Itametal®, compact model, Itabuna, BA, Brazil), with a 4 mm mesh, followed by refinement in a sieve with a 2 mm mesh. The pulps were placed in low-density polyethylene packaging and stored in a freezer with a controlled temperature of -18 ± 2 °C.

The mixed pulp was prepared by mixing equal parts of the whole jambolan and acerola pulps (1:1 ratio g g^{-1}) and homogenizing them in a domestic blender for 1 min. The foam mat drying process was performed after the preparation of three formulations: F1 (pulp + 1.0% albumin + 0.5% xanthan gum); F2 (pulp + 1.0% albumin + 0.5% CMC); F3 (pulp + 1.0% albumin + 0.5% guar gum). The foams were prepared by mixing the mixed pulp and additives in a mixer (Arno®, Deluxe, Itatiaia, RJ, Brazil) at maximum speed for different times determined in preliminary tests, F1 for 30 min; F2 for 20 min and F3 for 5 min.

Each foam produced from the formulations was spread, in triplicate, on stainless steel trays, making up a 0.5-cm-thick foam mat, measured with a digital caliper (Onebycitess). The samples in the trays were taken to dry in an oven with forced air circulation (FANEM, model 320E, São Paulo, SP, Brazil) with air speed of 1.0 m s^{-1}, at temperatures of 50, 60, 70 and 80 °C. During drying the trays were weighed at regular intervals until obtaining a constant mass. Three consecutive measurements were adopted as a criterion for determining the constant mass at regular 60 min intervals, with no change in the mass of the samples. The dry material was removed with a plastic spatula, and then crushed in a mini processor (Mallory, Oggi+, Maranguape, CE, Brazil). After that, it was stored in flexible laminated packaging (composed of a transparent PET layer, metallization and low-density polyethylene film - LDPE, with nominal total weight of 120 g m^{-2}, water vapor transmission rate of 5.38 g m^{-2} per day and oxygen permeability rate of 60 cm^3 m^{-2} per day) with dimensions of 10 × 17.5 cm. At the end of the drying, the dry masses were determined and the water content was calculated. With the obtaining of the experimental data, the values of the water content ratio were calculated (Eq. 1).

$$RX = \frac{(X - X_e)}{(X_0 - X_e)} \quad (1)$$

where:

RX - water content ratio of the product, dimensionless;
X - water content of the product at a given time, dry basis;
X_0 - initial water content of the product, dry basis; and,
X_e - equilibrium water content of the product, dry basis.

With the calculation of the water content ratio, curves of drying kinetics were plotted, represented by the water content ratio (dimensionless) as a function of drying time (min). For the selection of the most suitable models for the description of the foam mat drying process, 10 equations were fitted to the drying data (Table 1) frequently used to represent the drying kinetics (Moura et al., 2021; Omolola et al., 2019). The non-linear regression models using the Quasi-Newton estimation method were fitted using the computer software Statistics version 7.0.

The models were selected considering the magnitude of the coefficient of determination (R^2), the mean square deviation (MSD), Eq. 12, and the chi-square test (χ^2), Eq. 13.

Table 1. Non-linear regression models fitted to drying kinetics data

Model name	Model equation	Eq.
Page	$RX = \exp(-k.t^n)$	(2)
Henderson & Pabis	$RX = a.\exp(-k.t)$	(3)
Modified Henderson & Pabis	$RX = a.\exp(-k.t) + b.\exp(-k_0.t) + \exp(-k_1.t)$	(4)
Logarithmic	$RX = a.\exp(-k.t) + c$	(5)
Midilli	$RX = a.\exp(-k.t^n) + b.t$	(6)
Two-Term Exponential	$RX = a.\exp(-k.t) + (1-a)\exp(-k.a.t)$	(7)
Diffusion Approximation	$RX = a.\exp(-k.t) + (1-a)\exp(-k.b.t)$	(8)
Two Terms	$RX = a.\exp(-k_0.t) + b.\exp(-k_1.t)$	(9)
Newton	$RX = \exp(-k.t)$	(10)
Thompson	$RX = \exp((-a-(a^2 + 4.b.t)^{0.5})/2.b)$	(11)

RX - water content ratio of the product, dimensionless; k, k_0, k_1 - Drying constants, 1/min; a, a_0, b, c, n - Model constants (dimensionless); t - Drying time, in min

$$MSD = \frac{\sqrt{\sum\left(RX_{pred} - RX_{exp}\right)^2}}{n} \quad (12)$$

where:

MSD - mean square deviation;

RX_{pred} - water content ratio predicted by the model;

RX_{exp} - experimental water content ratio; and,

n - number of observations.

$$\chi^2 = \frac{\sum_{i=1}^{n}\left(RX_{pred} - RX_{exp}\right)^2}{DFR} \quad (13)$$

where:

RX_{exp} - experimental water content ratio;

RX_{pred} - water content ratio predicted by the model;

n - number of experimental observations; and,

DFR - degrees of freedom of the residual (number of experimental observations minus number of model coefficients).

The mathematical model of liquid diffusion (Eq. 14) fitted to the drying kinetics data for the mixed pulp formulations, which is the analytical solution for Fick's second law, and the effective diffusivity coefficients ($m^2\ s^{-1}$) for each temperature were obtained as follows.

$$RX = \frac{8}{\pi^2}\sum_{i=0}^{\infty}\frac{1}{(2i+1)^2}\exp\left[-(2i+1)^2\pi^2 D_{ef}\frac{t}{L^2}\right] \quad (14)$$

where:

RX - water content ratio of the product, dimensionless;

D_{ef} - effective diffusivity, $m^2\ s^{-1}$;

L - thickness of the drying layer, m;

i - number of terms; and,

t - drying time, s.

The flat plate geometry was used for the mixed pulp formulations, considering unidirectional movement of the water content, uniform distribution of the initial water content, whose water migrates only by diffusion, and that the external resistance and shrinkage are negligible, and the mathematical solution is represented by Eq. 14. To solve Eq. 14, the computer program Statistic version 7.0 was used through non-linear regression with the Quasi-Newton estimation method, with an approximation of four terms. The dependence of effective diffusivity (D_{ef}) with temperature was evaluated using an Arrhenius-type equation (Eq. 15), determining the activation energy (E_a).

$$D_{ef} = D_0\exp\left(\frac{E_a}{RT}\right) \quad (15)$$

where:

D_{ef} - effective diffusivity, $m^2\ s^{-1}$;

D_0 - pre-exponential factor, $m^2\ s^{-1}$;

E_a - activation energy, J mol^{-1};

R - universal gas constant, 8.314 J $mol^{-1}\ K^{-1}$; and,

T - absolute temperature, K.

The thermodynamic properties of enthalpy, entropy and Gibbs free energy of the drying process were calculated using Eqs. 16, 17 and 18, respectively.

$$\Delta H = E_a - RT \quad (16)$$

$$\Delta S = R\left[\ln(D_0) - \ln\left(\frac{K_B}{h_P}\right) - \ln(T)\right] \quad (17)$$

$$\Delta G = \Delta H - (T)\Delta S \quad (18)$$

where:

ΔG - Gibbs free energy, J mol^{-1};

ΔH - specific enthalpy, J mol^{-1};

ΔS - specific entropy, J mol^{-1} K;

k_B - Boltzmann constant, 1.38×10^{-23} J K^{-1};

h_P - Planck constant, 6.626×10^{-34} J s^{-1}; and,

T - absolute temperature, K.

Results and Discussion

Table 2 presents the drying time, powder yield and water content of samples F1, F2 and F3 subjected to foam mat drying at temperatures of 50, 60, 70 and 80 °C.

Table 2. Drying time, powder yield and water content of mixed pulp formulations in foam mat drying in the temperature range from 50 to 80 °C

Formulations	T (°C)	Drying time (min)	Powder yield (%)	Water content	
				(%)	(% db)
F1	50	510	9.71	12.07	13.73
	60	330	11.40	10.52	11.75
	70	300	10.63	9.04	9.94
	80	270	10.83	9.19	10.13
F2	50	510	11.00	13.70	15.88
	60	450	11.28	13.16	15.16
	70	330	11.27	12.64	14.47
	80	270	10.21	9.29	10.25
F3	50	390	10.53	13.46	15.56
	60	270	10.93	12.69	14.54
	70	210	11.36	10.95	12.30
	80	180	11.65	8.27	9.01

db - Dry basis. Formulations: F1 - Albumin (1.0%) + Xanthan gum (0.5%); F2 - Albumin (1.0%) + Sodium carboxymethyl cellulose (0.5%); F3 - Albumin (1.0%) + Guar gum (0.5%)

The progressive reductions observed showed, over the drying time, temperature increases in the three formulations, with similar times between formulations F1 and F2 and a more marked reduction in the times of the formulation containing guar gum, F3, at all drying temperatures. The increase of 30 °C reduced the total drying time by 47% in formulations F1 and F2, and by 54% in formulation F3.

The drying performance showed little variation between formulations and applied temperatures, while the water content decreased between temperatures, but in different percentages between subsequent temperatures according to each formulation, with the lowest value in formulation F3.

Cuevas et al. (2019) also reported final water content of 10%, drying olive biomasses at six different temperatures, between 70 and 120 °C. Tan & Sulaiman (2019) studied the foam mat drying kinetics of *Hibiscus sabdariffa* L. at 50 °C, reporting a time of 360 min to reach a final water content of 5 to 7%. Tavares et al. (2019), studying the foam mat drying of BRS Violet grape at different temperatures, observed 52% reduction of drying time with the increase from 60 to 80 °C, with these powder products obtained after 375 and 160 min, respectively.

Table 3 presents the parameters of the models fitted to the drying kinetics data of formulation F1, with the respective

Table 3. Parameters, coefficients of determination (R^2), chi-squares (χ^2) and mean square deviations (MSD) of the models fitted to the drying data of formulation F1 (1.0% albumin + 0.5% xanthan gum) with 0.5-cm-thick foam mat

Model	T (°C)	Parameters						R^2	χ^2	MSD
Modified Henderson & Pabis		a	k	b	k_0	c	k_1			
	50	0.3542	0.0087	0.3542	0.0087	0.354	0.008	0.9850	0.0027	0.0454
	60	0.3616	0.0130	0.3616	0.0130	0.3616	0.0131	0.9829	0.0033	0.0490
	70	0.3615	0.0157	0.3615	0.0157	0.3615	0.0157	0.9814	0.0036	0.0509
	80	0.3612	0.0173	0.3612	0.0173	0.3612	0.0173	0.9844	0.0030	0.0460
Midilli		a	b	n	k	-	-			
	50	0.9776	-0.00005	1.3627	0.0013	-	-	0.9979	0.0003	0.0171
	60	0.9817	-0.00004	1.4618	0.0015	-	-	0.9990	0.0002	0.0118
	70	0.9745	-0.00005	1.4916	0.0017	-	-	0.9978	0.0004	0.0174
	80	0.9821	-0.00004	1.4383	0.0025	-	-	0.9990	0.0002	0.0114
Two terms		a	k_0	k_1	b	-	-			
	50	0.5320	0.0088	0.0088	0.5320	-	-	0.9849	0.0025	0.0456
	60	0.5420	0.0131	0.0131	0.5429	-	-	0.9829	0.0029	0.0490
	70	0.5413	0.0157	0.0157	0.5436	-	-	0.9814	0.0032	0.0509
	80	0.5427	0.0173	0.0173	0.5412	-	-	0.9844	0.0026	0.0460
Diffusion approximation		a	b	k	-	-	-			
	50	-261.9565	0.9971	0.0156	-	-	-	0.9964	0.0006	0.0222
	60	-256.4889	0.9966	0.0245	-	-	-	0.9976	0.0004	0.0184
	70	-285.0497	0.9970	0.0291	-	-	-	0.9959	0.0007	0.0239
	80	-137.2101	0.9939	0.0320	-	-	-	0.9979	0.0003	0.0170
Logarithmic		a	k	c	-	-	-			
	50	1.1351	0.0072	-0.0910	-	-	-	0.9917	0.0013	0.0338
	60	1.1503	0.0110	-0.0852	-	-	-	0.9997	0.0017	0.0380
	70	1.1426	0.0134	-0.0758	-	-	-	0.9979	0.0020	0.0410
	80	1.1386	0.0148	-0.0728	-	-	-	0.9904	0.0015	0.0361
Page		k	n	-	-	-	-			
	50	0.0016	1.3339	-	-	-	-	0.9967	0.0005	0.0212
	60	0.0018	1.4271	-	-	-	-	0.9984	0.0002	0.0148
	70	0.0024	1.4231	-	-	-	-	0.9970	0.0005	0.0204
	80	0.0030	1.4006	-	-	-	-	0.9986	0.0002	0.0139
Henderson & Pabis		a	k	-	-	-	-			
	50	1.0624	0.0087	-	-	-	-	0.9850	0.0022	0.0454
	60	1.0849	0.0131	-	-	-	-	0.9829	0.0026	0.0490
	70	1.0850	0.0157	-	-	-	-	0.9814	0.0029	0.0509
	80	1.0839	0.0173	-	-	-	-	0.9844	0.0024	0.0460
Thompson		a	b	-	-	-	-			
	50	-2953.10	1.8446	-	-	-	-	0.9793	0.0031	0.0533
	60	-3031.15	1.8945	-	-	-	-	0.9738	0.0040	0.0606
	70	-2118.03	1.8755	-	-	-	-	0.9729	0.0042	0.0614
	80	-2474.88	1.9018	-	-	-	-	0.9761	0.0036	0.0570
Two-term exponential		a	k	-	-	-	-			
	50	0.0020	3.9903	-	-	-	-	0.9790	0.0031	0.0538
	60	0.0019	6.1372	-	-	-	-	0.9734	0.0041	0.0611
	70	0.0018	7.8485	-	-	-	-	0.9725	0.0042	0.0619
	80	0.0021	7.5546	-	-	-	-	0.9756	0.0037	0.0575
Newton		k	-	-	-	-	-			
	50	0.0080	-	-	-	-	-	0.9793	0.0030	0.0533
	60	0.0118	-	-	-	-	-	0.9738	0.0038	0.0606
	70	0.0142	-	-	-	-	-	0.9729	0.0040	0.0614
	80	0.0157	-	-	-	-	-	0.9761	0.0034	0.0570

coefficients of determination (R^2), chi-squares (χ^2) and mean square deviations (MSD).

It was verified that the increase in temperature increases the k parameter values. The drying constant k can be used as an approximation to characterize the temperature effect, tending to increase with it, since high temperatures lead to higher drying rates, reaching the equilibrium water content faster. An increase in the drying constant (k) was also observed with increases in drying temperature (50-80 °C) for the Midilli, Diffusion Approximation, Henderson & Pabis, and Newton models for the trapiá peel residues (Moura et al., 2021). Parameter n has a moderating effect on time and corrects the likely errors resulting from the neglect of internal resistance to water transfer (Mendonça et al., 2019).

The fitted models showed high values of coefficients of determination ($R^2 \geq 0.97$), low values of chi-square ($\chi^2 \leq 0.004$) and mean square deviations (MSD ≤ 0.06) at the evaluated temperatures, indicating high proximity between the values estimated by the models and the experimental data. In many studies with drying of fruit pulps, similar values of R^2 between different models make MSD the criterion of choice for the selection of the best fits (Feitosa et al., 2017; Santos et al., 2019b).

The selection and recommendation of the best model are based on the values of R^2, χ^2 and MSD. With good fits by the Page, Diffusion approximation and Logarithmic models, the Midilli model showed the set of higher R^2 values and lower χ^2 and MSD, which are the best performance criteria for the representation of the drying kinetics of the F1 formulation.

Studying the drying of trapiá (*Crataeva tapia* L.) peel residues, Moura et al. (2021) fitted 10 models to the drying data, obtaining better results with the Midilli model. Vimercati et al. (2019) found the highest R^2 value and the lowest standard error with the Page model for the foam mat drying of strawberry (*Fragaria* sp.) pulp. Likewise, Mphahlele et al. (2019) found that the Midilli model more accurately represented the drying characteristics of foam mat (0.5 cm) of pomegranate peel in the range of 40 to 60 °C, with the highest value of R^2 compared to the other drying models.

The drying kinetics data of the F1 formulation (Figure 1) shows fits of the curves by the Midilli model.

Among the curves, the distancing of the curve for 50 °C from the others stands out, which is the result of more pronounced drying rates at temperatures above 60 °C, observed for smaller increments up to 80 °C.

Morais et al. (2019) showed that, at the beginning of drying, the surface moisture of the product is easily eliminated, which justifies the higher drying rates. However, as the dehydration process continues, the moisture located inside the sample must move to the surface, resulting in resistance to diffusion and reduction in the drying rate. The drying rate increases as the temperature is raised until the surface temperature reaches its equilibrium. Galdino et al. (2016) showed the influence of temperature on the drying curves of whole atemoya pulp, which indicates that the higher the temperature, the faster the drying.

The values of the coefficient of determination ($R^2 \geq 0.97$), chi-squares ($\chi^2 \leq 0.009$) and the mean square deviations (DSM ≤ 0.08) of the models fitted to the drying kinetics data of the F2 formulation (Table 4) demonstrate better results achieved with Midilli, Diffusion Approximation, Logarithmic and Page models, at the four temperatures tested.

Morais et al. (2019) obtained R^2 values above 0.99 when fitting the models of Midilli, Logarithmic and Page to the drying data of bacaba (*Oenocarpus bacaba* Mart.) pulp, at temperatures of 40, 50 and 60 °C. Santos et al. (2019b), studying drying of acuri (*Attalea phalerata* Mart. ex Spreng.) in slices, fitted five models to the data and noted that the Midilli and Logarithmic models equally fitted the data with a high degree of precision.

There was also increase in the drying constant k with increasing temperature for formulation F2, indicating that the greater the magnitude of k, the greater the effective diffusivity in the drying process. With the best performance criteria, R^2, χ^2 and MSD, the Midilli model was used to fitting to the drying kinetics of formulation F2 (Figure 2).

As observed in formulation F1, temperatures from 60 to 80 °C stand out from 50 °C, revealing a more proportional correspondence between temperature increases and the drying rate, with a less efficient response of drying at 50 °C.

In other agricultural products, the Midilli model also provided good fits to the drying kinetics data, as reported by

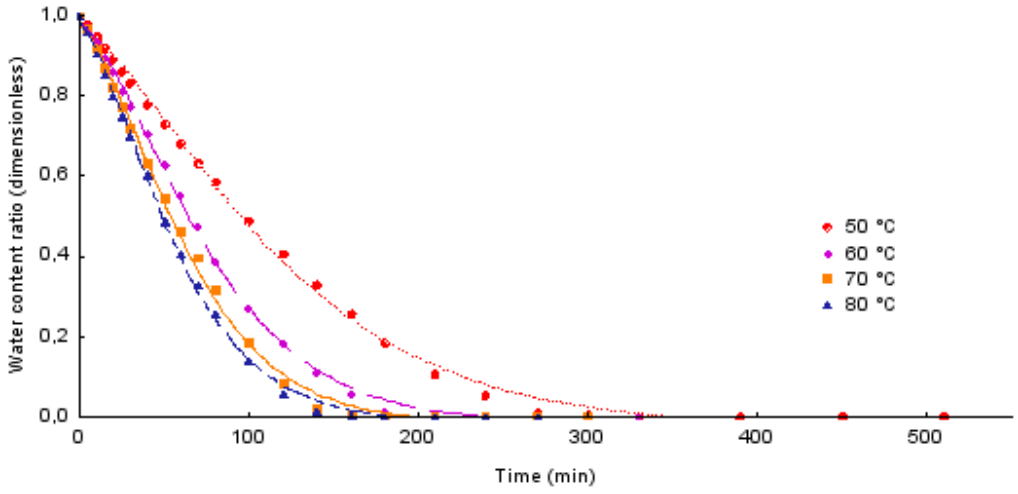

Figure 1. Water content ratio as a function of foam mat drying time for formulation F1 in the temperature range from 50 to 80 °C with fits of the Midilli model

Table 4. Parameters, coefficients of determination (R^2), chi-squares (χ^2) and mean square deviations (MSD) of the models fitted to the drying data of formulation F2 (1.0% albumin + 0.5% CMC) with 0.5-cm-thick foam mat

Model	T (°C)	Parameters						R^2	χ^2	MSD
		a	k	b	K_0	c	K_1			
Modified Henderson & Pabis	50	0.3507	0.0077	0.3507	0.0077	0.3507	0.0077	0.9954	0.0098	0.0862
	60	0.3550	0.0106	0.3550	0.0106	0.3550	0.0106	0.9874	0.0023	0.0415
	70	0.3552	0.0122	0.3552	0.0122	0.3552	0.0122	0.9873	0.0023	0.0410
	80	0.3598	0.0146	0.3598	0.0146	0.3598	0.0146	0.9825	0.0034	0.0485
		a	b	n	k	-	-			
Midilli	50	0.9862	-0.0004	1.2754	0.0018	-	-	0.9997	0.0001	0.0092
	60	0.9790	-0.0004	1.3593	0.0018	-	-	0.9987	0.0002	0.0134
	70	0.9802	-0.0006	1.3455	0.0023	-	-	0.9989	0.0002	0.0123
	80	0.9793	-0.0007	1.4336	0.0020	-	-	0.9988	0.0002	0.0124
		a	K_0	K_1	b	-	-			
Two Terms	50	0.5135	0.0077	0.0077	0.5398	-	-	0.9954	0.0014	0.0343
	60	0.5339	0.0106	0.0106	0.5311	-	-	0.9874	0.0021	0.0415
	70	0.5328	0.0122	0.0122	0.5328	-	-	0.9873	0.0021	0.0410
	80	0.5407	0.0184	0.0184	0.5407	-	-	0.9823	0.0030	0.0490
		a	b	k	-	-	-			
Diffusion Approximation	50	-111.2881	0.9937	0.0135	-	-	-	0.9994	0.0002	0.0120
	60	-192.0346	0.9960	0.0189	-	-	-	0.9977	0.0004	0.0178
	70	-213.6552	0.9965	0.0217	-	-	-	0.9978	0.0003	0.0171
	80	-183.2581	0.9954	0.0341	-	-	-	0.9966	0.0005	0.0214
		a	k	c	-	-	-			
Logarithmic	50	1.1244	0.0064	-0.088	-	-	-	0.9980	0.0006	0.0227
	60	1.1223	0.0091	-0.074	-	-	-	0.9929	0.0011	0.0312
	70	1.1349	0.0101	-0.090	-	-	-	0.9940	0.0009	0.0282
	80	1.1645	0.0117	-0.108	-	-	-	0.9912	0.0014	0.0344
		k	n	-	-	-	-			
Page	50	0.0020	1.2609	-	-	-	-	0.9994	0.0002	0.0126
	60	0.0023	1.3216	-	-	-	-	0.9979	0.0003	0.0170
	70	0.0028	1.3159	-	-	-	-	0.9980	0.0003	0.0162
	80	0.0024	1.3987	-	-	-	-	0.9980	0.0003	0.0164
		a	k	-	-	-	-			
Henderson & Pabis	50	1.0533	0.0077	-	-	-	-	0.9931	0.0019	0.0421
	60	1.0650	0.0106	-	-	-	-	0.9818	0.0027	0.0500
	70	1.0656	0.0122	-	-	-	-	0.9814	0.0027	0.0496
	80	1.0799	0.0146	-	-	-	-	0.9739	0.0039	0.0596
		a	b	-	-	-	-			
Thompson	50	-2960.633	1.8288	-	-	-	-	0.9931	0.0019	0.0421
	60	-2684.087	1.8587	-	-	-	-	0.9818	0.0027	0.0500
	70	-2514.453	1.8681	-	-	-	-	0.9814	0.0027	0.0496
	80	-2579.676	1.8894	-	-	-	-	0.9739	0.0039	0.0596
		a	k	-	-	-	-			
Two-term Exponential	50	0.0020	3.5806	-	-	-	-	0.9929	0.0015	0.0343
	60	0.0019	5.1059	-	-	-	-	0.9814	0.0028	0.0504
	70	0.0020	5.5505	-	-	-	-	0.9811	0.0028	0.0501
	80	0.0019	6.8457	-	-	-	-	0.9735	0.0040	0.0596
		k	-	-	-	-	-			
Newton	50	0.0072	-	-	-	-	-	0.9931	0.0018	0.0421
	60	0.0098	-	-	-	-	-	0.9818	0.0026	0.0500
	70	0.0113	-	-	-	-	-	0.9815	0.0026	0.0496
	80	0.0132	-	-	-	-	-	0.9739	0.0037	0.0592

Zhou et al. (2019) studying the foam mat drying kinetics (60, 70 and 80 °C) of peach pulp; by Santos et al. (2019a) in the drying of patauá (*Oenocarpus bataua* Mart.) pulp at different temperatures (40, 50 and 60 °C) and foam mat thicknesses (0.3 and 0.6 cm).

The fits to the drying kinetics data of the F3 formulation (Table 5) resulted in high values of coefficients of determination (R^2), ranging from 0.97 to 0.99, chi-squares (χ^2) less than 0.005 and mean square deviations (MSD) less than 0.07. From the set of performance criteria, the Midilli model showed higher coefficients of determination (R^2), and lower MSD and χ^2.

Araújo et al. (2017) working with foam mat drying of acerola (*Malpighia emarginata* D.C.) also found that the models by Page, Newton and Henderson & Pabis showed satisfactory fits to the experimental data.

The drying data of formulation F3 (Figure 3) shows the fitting curves by the model of Midilli. Note the similarity in the behavior of the drying curves of formulation F3 with that of formulations F1 and F2, in which the curve at 50 °C is distant from the behavior of drying curves from 60 to 80 °C, indicating that the increase of 10 °C in the drying temperature between 50 and 60 °C was more effective in increasing the drying rate than the 10 °C interval increases between 60 and 80 °C, whose curves indicate more progressive rate increases.

The effective diffusivity coefficient (D_{ef}) is the mass diffusional parameter in Fick's law, and it represents the

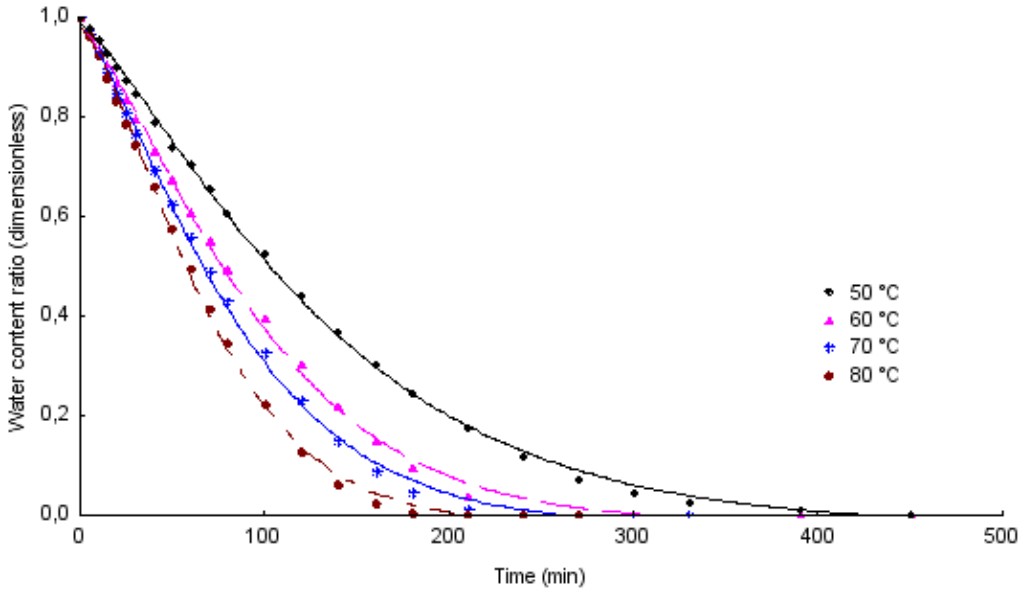

Figure 2. Water content ratio as a function of foam mat drying time for formulation F2 in the temperature range from 50 to 80 °C with fits using the Midilli model

Table 5. Parameters, coefficients of determination (R^2), chi-squares (χ^2) and mean square deviations (MSD) of the models fitted to the drying data of formulation F3 (1.0% albumin + 0.5% guar gum) with 0.5-cm-thick foam mat

Model	T (°C)	Parameters						R^2	χ^2	MSD
Modified Henderson & Pabis		a	k	b	K_0	c	K_1			
	50	0.3531	0.0111	0.3531	0.0111	0.3531	0.0111	0.9858	0.0026	0.0437
	60	0.3611	0.0155	0.3611	0.0155	0.3611	0.0155	0.9829	0.0033	0.0482
	70	0.3544	0.0182	0.3544	0.0182	0.3544	0.0182	0.9804	0.0037	0.0498
	80	0.3616	0.0206	0.3616	0.0207	0.3616	0.0207	0.9810	0.0038	0.0495
Midilli		a	b	n	k	-	-			
	50	0.9754	-0.001	1.3448	0.0020	-	-	0.9982	0.0003	0.0156
	60	0.9811	-0.001	1.4406	0.0021	-	-	0.9990	0.0002	0.0118
	70	0.9616	-0.001	1.4317	0.0027	-	-	0.9971	0.0005	0.0193
	80	0.9841	-0.001	1.4247	0.0034	-	-	0.9986	0.0002	0.0136
Two Terms		a	K_0	K_1	b	-	-			
	50	0.5255	0.0111	0.0111	0.5340	-	-	0.9858	0.0023	0.0437
	60	0.5416	0.0155	0.0155	0.5416	-	-	0.9829	0.0029	0.0482
	70	0.5317	0.0183	0.0183	0.5317	-	-	0.9804	0.0032	0.0498
	80	0.5426	0.0207	0.0207	0.5426	-	-	0.9810	0.0032	0.0495
Diffusion Approximation		a	b	k	-	-	-			
	50	-215.20	0.9965	0.0197	-	-	-	0.9968	0.0005	0.0208
	60	-239.68	0.9965	0.0286	-	-	-	0.9975	0.0004	0.0186
	70	-259.03	0.9970	0.0327	-	-	-	0.9945	0.0008	0.0264
	80	-208.48	0.9959	0.0382	-	-	-	0.9969	0.0005	0.0201
Logarithmic		a	k	c	-	-	-			
	50	1.1292	0.0092	-0.090	-	-	-	0.9926	0.0011	0.0315
	60	1.1565	0.0127	-0.095	-	-	-	0.9907	0.0015	0.0356
	70	1.1541	0.0144	-0.116	-	-	-	0.9904	0.0015	0.0349
	80	1.1759	0.0163	-0.117	-	-	-	0.9909	0.0014	0.0343
Page		k	n	-	-	-	-			
	50	0.0025	1.3152	-	-	-	-	0.9969	0.0005	0.0204
	60	0.0025	1.4067	-	-	-	-	0.9983	0.0003	0.0153
	70	0.0042	1.3468	-	-	-	-	0.9950	0.0007	0.0252
	80	0.0038	1.4079	-	-	-	-	0.9978	0.0003	0.0168
Henderson & Pabis		a	k	-	-	-	-			
	50	1.0594	0.0111	-	-	-	-	0.9858	0.0021	0.0437
	60	1.0832	0.0155	-	-	-	-	0.9829	0.0026	0.0482
	70	1.0635	0.0183	-	-	-	-	0.9804	0.0028	0.0498
	80	1.0851	0.0207	-	-	-	-	0.9810	0.0028	0.0495
Thompson		a	b	-	-	-	-			
	50	-2731.73	1.8672	-	-	-	-	0.9809	0.0028	0.0506
	60	-2285.96	1.8824	-	-	-	-	0.9740	0.0039	0.0593
	70	-2243.97	1.8999	-	-	-	-	0.9749	0.0036	0.0563
	80	-1750.96	1.8850	-	-	-	-	0.9717	0.0041	0.0605

Continues on the next page

Continuation of Table 5

Model	T (°C)	Parameters						R^2	χ^2	MSD
		a	k	-	-	-	-			
Two-Term Exponential	50	0.0020	5.0296	-	-	-	-	0.9805	0.0029	0.0511
	60	0.0018	7.5819	-	-	-	-	0.9736	0.0040	0.0598
	70	0.0021	8.1843	-	-	-	-	0.9746	0.0036	0.0567
	80	0.0020	9.4963	-	-	-	-	0.9712	0.0042	0.0610
		k	-	-	-	-	-			
Newton	50	0.0103	-	-	-	-	-	0.9809	0.0027	0.0506
	60	0.0140	-	-	-	-	-	0.9740	0.0037	0.0593
	70	0.0169	-	-	-	-	-	0.9749	0.0034	0.0563
	80	0.0187	-	-	-	-	-	0.9717	0.0039	0.0605

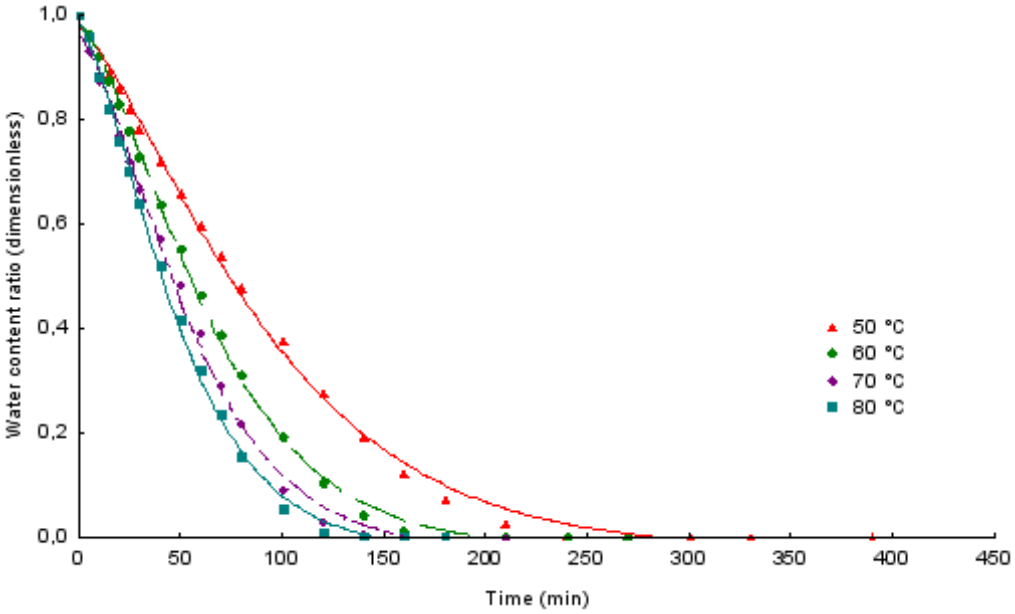

Figure 3. Water content ratio as a function of foam mat drying time for formulation F3 in the temperature range from 50 to 80 °C with fits of the Midilli model

conductive term of the entire moisture transfer mechanism inside the product, such as molecular diffusion, capillary flow, Knudsen flow and hydrodynamic flow (Castro et al., 2018). Table 6 shows the values of the effective diffusion coefficients of the three mixed pulp formulations, at drying temperatures from 50 to 80 °C, obtained by applying the liquid diffusion model.

As the drying temperature increased, there was increase in the effective water diffusivity of the samples, corresponding to increases of 98.06, 87.51 and 84.15% in formulations F1, F2 and F3, respectively, comparing the extremes of temperatures. The F1 sample showed the greatest increase in diffusivity among the samples; however, the F3 sample started from a higher diffusivity at 50 °C, so this formulation had the highest value, among the three evaluated, at 80 °C. An increase in temperature causes a reduction in water viscosity and increases the mobility of the liquid's molecules (Touil et al., 2014).

Table 6. Effective diffusivity coefficients (D_{ef}) and coefficients of determination (R^2) obtained in the drying kinetics of the formulations at temperatures of 50, 60, 70 and 80 °C

Formulation	T (°C)	D_{ef} ($m^2\ s^{-1}$)	R^2
F1	50	2.580×10^{-10}	0.9204
	60	3.843×10^{-10}	0.9118
	70	4.644×10^{-10}	0.9143
	80	5.110×10^{-10}	0.9178
F2	50	2.291×10^{-10}	0.9267
	60	3.162×10^{-10}	0.9258
	70	3.637×10^{-10}	0.9236
	80	4.296×10^{-10}	0.9101
F3	50	3.325×10^{-10}	0.9248
	60	4.550×10^{-10}	0.9116
	70	5.527×10^{-10}	0.9175
	80	6.123×10^{-10}	0.9079

F1 - Albumin (1.0%) + Xanthan gum (0.5%); F2 - Albumin (1.0%) + Sodium carboxymethyl cellulose (0.5%); F3 - Albumin (1.0%) + Guar gum (0.5%)

Similar behavior of increasing D_{ef} as the drying temperature increases was verified by Dehghannya et al. (2019) in the foam mat drying (50, 60 and 70 °C) of lemon (*Citrus latifolia*) juice, due to the increase in vapor pressure inside the foam as a result of the higher temperatures, with D_{ef} results between 1.061×10^{-8} and 1.666×10^{-8} $m^2\ s^{-1}$, and by Freitas et al. (2018), in the of drying of yellow mombin (*Spondias mombin* L.) pulp, with effective diffusivity between 5.18×10^{-9} and 2.68×10^{-8} $m^2\ s^{-1}$ between temperatures from 50 to 80 °C. Sousa et al. (2017) studied the effective diffusivities in dried pequi (*Caryocar coriaceum* Wittm) pulps in layers with thicknesses of 0.5, 1.0 and 1.5 cm, at 50, 60, 70 and 80 °C, and reported increases in diffusivity values with increasing layer thickness and temperature, with values ranging between 0.93 and 3.93×10^{-8} $m^2\ s^{-1}$.

The effect of drying temperature on effective diffusivity is generally explained using an Arrhenius equation, to obtain a better agreement between experimental and predicted data

Table 7. Values of the parameters of the Arrhenius equation, activation energy (E_a) and coefficient of determination (R^2) of mixed pulp formulations at temperatures from 50 to 80 °C

Formulation	D_0 ($m^2\ s^{-1}$)	E_a (kJ mol^{-1})	R^2
F1	7.99×10^{-7}	21.3923	0.8922
F2	3.13×10^{-7}	19.2795	0.9545
F3	4.63×10^{-7}	19.3183	0.9390

F1 - Albumin (1.0%) + Xanthan gum (0.5%); F2 - Albumin (1.0%) + Sodium carboxymethyl cellulose (0.5%); F3 - Albumin (1.0%) + Guar gum (0.5%)

(Moura et al., 2021). Thus, Table 7 shows the activation energy values for the effective diffusivity in the drying process of F1, F2 and F3 formulations in the temperature range between 50 and 80 °C.

Zogzas et al. (1996) state that the activation energy for effective diffusivity in the agricultural products varies from 12.7 to 110 kJ mol^{-1}, a range which encompasses the activation energies determined in the drying of mixed pulp formulations. The results show that F1 required greater activation energy for the drying process and that the other formulations showed values close to each other.

Mohammadi et al. (2018) reported an activation energy value of 29.93 kJ mol^{-1} in a kiwi fruit drying test. Komolafe et al. (2019), studying the solar drying of locust beans (*Parkia biglobosa*), determined activation energy value of 21.65 kJ mol^{-1}. The high E_a value implies a great need for energy, since a higher barrier must be overcome to start the water release process.

Table 8 shows the values the thermodynamic properties with the values of the enthalpy (ΔH), entropy (ΔS) and Gibbs free energy (ΔG) for F1, F2 and F3 formulations subjected to drying at temperatures between 50 and 80 °C.

The ΔH values were positive indicating that in the foam mat drying process, heat is absorbed by the sample through heat transfer, that is, it is an endothermic process. With the increase in the drying temperature, there was reduction in the values of enthalpy.

The ΔH values for the mixed pulp ranged between 16.3447 and 18.7069 kJ mol^{-1}, being lower than those of the convective drying of bacaba pulp (34.2391 to 34.4054 kJ mol^{-1}) for temperatures between 40 and 60 °C (Morais et al., 2019). These differences are probably due to the chemical composition of the pulps, temperatures and the type of drying process, as foam mat drying favors the release of water, hence requiring less energy to remove water from the product. It is observed that among the three formulations F2 had the lowest values of ΔH, followed by F3 and F1, indicating that F2 needs less energy to dry.

Table 8. Thermodynamic properties, enthalpy (ΔH), entropy (ΔS) and Gibbs free energy (ΔG), of drying kinetics of mixed pulp formulations at temperatures of 50, 60, 70 and 80 °C

Formulation	T (°C)	ΔH (kJ mol^{-1})	ΔS (kJ mol^{-1} K^{-1})	ΔG (kJ mol^{-1})
F1	50	18.7069	-0.3623	135.7289
	60	18.6237	-0.3626	139.3532
	70	18.5406	-0.3628	142.9799
	80	18.4575	-0.3630	146.6091
F2	50	16.5941	-0.3701	136.1286
	60	16.5109	-0.3703	139.8306
	70	16.4278	-0.3706	143.5352
	80	16.3447	-0.3708	147.2421
F3	50	16.6329	-0.3668	135.1172
	60	16.5497	-0.3671	138.7867
	70	16.4666	-0.3673	142.4587
	80	16.3835	-0.3676	146.1332

F1 - Albumin (1.0%) + Xanthan gum (0.5%); F2 - Albumin (1.0%) + Sodium carboxymethyl cellulose (0.5%); F3 - Albumin (1.0%) + Guar gum (0.5%)

The entropy has been reduced with the increase in the drying temperature, indicating that the lower the entropy, the lower the excitation of the water molecules, that is, there is a greater degree of order between the water molecules and the product (Silva et al., 2016).

Gibbs free energy characterizes the drying process as spontaneous or non-spontaneous and indicates how much water is bound to the product. Gibbs free energy increased with increasing drying temperature and the positive sign (ΔG > 0) indicates that the reaction was endergonic, that is, non-spontaneous, in which the addition of energy from the surrounding air is necessary for the withdrawal of water from the product.

Silva et al. (2016), determining the thermodynamic parameters of the anthocyanin thermal degradation in acerola (*Malpighia emarginata* D.C.) pulp, found lower Gibbs free energy values (86.670 to 88.603 kJ mol^{-1}) for temperatures between 60 and 90 °C.

Santos et al. (2019a) observed reduction in enthalpy (29.8025 to 29.6363 kJ mol^{-1}) and an increase in entropy (-0.3246 to -0.3251 kJ mol^{-1} K^{-1}) and Gibbs free energy (131.4560 to 137.9535 kJ mol^{-1}) in the drying of patauá (*Oenocarpus bataua* Mart.) pulp under different temperatures (40, 50 and 60 °C) in the 0.6-cm-thick foam mat.

Conclusions

1. Samples of jambolan and acerola mixed pulp with addition of albumin + guar gum (F3) dried in shorter times, followed by samples with albumin + xanthan gum (F1). The drying models applied satisfactorily fitted the drying kinetics of the samples in the temperature range from 50 to 80 °C, with better performance by the Midilli model.

2. The effective diffusivity coefficients showed higher values in the samples of formulation with jambolan and acerola mixed pulp and additives albumin + gum guar (F3). The activation energy was higher in the pulp formulation using albumin + xanthan gum (F1), while samples with addition of albumin + sodium carboxymethyl cellulose (F2) and albumin + gum guar (F3) were equivalent.

3. Enthalpy and entropy decreased with drying temperature, and Gibbs free energy increased; the greatest enthalpy and entropy were determined in the samples with albumin + guar gum (F3) and the highest Gibbs free energy in the samples with albumin + xanthan gum (F1).

4. The elevation of the drying air temperature caused greater reduction in the water content and in the dehydration time of the samples.

Literature Cited

Araújo, C. da S.; Macedo, L. L.; Vimercati, W. C.; Saraiva, S. H.; Oliveira, A. do N.; Teixeira, L. J. Q. Cinética de secagem de acerola em leito de espuma e ajuste de modelos matemáticos. Brazilian Journal of Food Technology, v.20, p.1-9, 2017. https://doi.org/10.1590/1981-6723.15216

Castro, A. M.; Mayorga, E. Y.; Moreno, F. L. Mathematical modelling of convective drying of fruits: a review. Journal of Food Engineering, v.223, p.152-167, 2018. https://doi.org/10.1016/j.jfoodeng.2017.12.012

Chhikara, N.; Kaur, R.; Jaglan, S.; Sharma, P.; Gat, Y.; Panghal, A. Bioactive compounds, pharmacological and food application of *Syzygium cumini* - A review. Food & Function, v.9, p.6096-6115, 2018. https://doi.org/10.1039/C8FO00654G

Cuevas, M.; Martínez-Cartas, M. L.; Pérez-Villarejo, L.; Hernández, L.; García-Martín, J. F.; Sánchez, S. Drying kinetics and effective water diffusivities in olive stone and olive-tree pruning. Renewable Energy, v.132, p.911-920, 2019. https://doi.org/10.1016/j.renene.2018.08.053

Dehghannya, J.; Pourahmad, M.; Ghanbarzadeh, B.; Ghaffari, H. A multivariable approach for intensification of foam-mat drying process: Empirical and three-dimensional numerical analyses. Chemical Engineering and Processing, v.135, p.22-41, 2019. https://doi.org/10.1016/j.cep.2018.11.010

Feitosa, R. M.; Figueirêdo, R. M. F. de; Queiroz, A. J. de M.; Lima, F. C. dos S.; Oliveira, E. N. A. de. Drying and characterization of myrtle pulp. Revista Brasileira de Engenharia Agrícola e Ambiental, v.21, p.858-864, 2017. https://doi.org/10.1590/1807-1929/agriambi.v21n12p858-864

Freitas, B. S. M. de.; Cavalcante, M. D.; Cagnin, C.; Silva, R. M. da; Plácido, G. R.; Oliveira, D. E. C. de. Physical-chemical characterization of yellow mombin (*Spondias mombin* L.) foam-mat drying at different temperatures. Revista Brasileira de Engenharia Agrícola e Ambiental, v.22, p.430-435, 2018. https://doi.org/10.1590/1807-1929/agriambi.v22n6p430-435

Galdino, P. O.; Figueirêdo, R. M. F. de; Queiroz, A. J. de M.; Galdino, P. O. Drying kinetics of atemoya pulp. Revista Brasileira de Engenharia Agrícola e Ambiental, v.20, p.672-677, 2016. https://doi.org/10.1590/1807-1929/agriambi.v20n7p672-677

Komolafe, C. A.; Ojediran, J. O.; Ajao, F. O.; Dada, O. A.; AfolabI, Y. T.; Oluwaleye, I. O.; Alake, A. S. Modelling of moisture diffusivity during solar drying of locust beans with thermal storage material under forced and natural convection mode. Case Studies in Thermal Engineering, v.15, p.1-11, 2019. https://doi.org/10.1016/j.csite.2019.100542

Mendonça, A. P.; Silva, L. M. de M.; Sousa, F. C. de; Silva, J. R. da; Rosa, J. C. Modelagem matemática das curvas de secagem de sementes de duas espécies de andiroba. Revista Engenharia na Agricultura, v.27, p.293-303, 2019. https://doi.org/10.13083/reveng.v27i4.888

Mohammadi, I.; Tabatabaekoloor, R.; Motevali, A. Effect of air recirculation and heat pump on mass transfer and energy parameters in drying of kiwifruit slices. Energy, v.170, p.149-158, 2018. https://doi.org/10.1016/j.energy.2018.12.099

Morais, M. F. de; Santos, J. R. O. dos; Santos, M. P.; Santos, D. da C.; Costa, T. N. da; Lima, J. B. Modeling and thermodynamic properties of 'bacaba' pulp drying. Revista Brasileira de Engenharia Agrícola e Ambiental, v.23, p.702-708, 2019. https://doi.org/10.1590/1807-1929/agriambi.v23n9p702-708

Moreira, I. dos S.; Silva, W. P. da; Castro, D. S. de; Silva, L. M. M.; Gomes, J. P.; Silva, C. M. D. P. S. e. Production of kiwi snack slice with different thickness: drying kinetics, sensory and physicochemical analysis. Australian Journal of Crop Science, v.12, p.778-787, 2018. https://doi.org/10.21475/ajcs.18.12.05.PNE925

Moura, H. V.; Figueirêdo, R. M. F. de; Queiroz, A. J. de M.; Silva, E. T. V.; Esmero, J. A. D.; Lisbôa, J. F.; Mathematical modeling and thermodynamic properties of the drying kinetics of trapia residues. Journal of Food Process Engineering, v.44, p.1-11, 2021. https://doi.org/10.1111/jfpe.13768

Mphahlele, R. R.; Pathare, P. B.; Opara, U. L. Drying kinetics of pomegranate fruit peel (cv. wonderful). Scientific African, v.5, p.1-8, 2019. https://doi.org/10.1016/j.sciaf.2019.e00145

Nogueira, G. D. R.; Silva, P. B.; Duarte, C. R.; Barrozo, M. A. S. Analysis of a hybrid packed bed dryer assisted by infrared radiation for processing acerola (*Malpighia emarginata* D.C.) residue. Food and Bioproducts Processing, v.114, p.235-244, 2019. https://doi.org/10.1016/j.fbp.2019.01.007

Omolola, A. O.; Kapila, P. F.; Silungwe, H. Drying and colour characteristics of *Cleome gynandra* L. (spider plant) leaves. Food Science and Technology, v.39, p.588-594, 2019. https://doi.org/10.1590/fst.27118

Panghal, A.; Kaur, R.; Janghu, S.; Sharma, P.; Sharma, P.; Chhikara, N. Nutritional, phytochemical, functional and sensorial attributes of *Syzygium cumini* L. pulp incorporated pasta. Food Chemistry, v.289, p.723-728, 2019. https://doi.org/10.1016/j.foodchem.2019.03.081

Santos, D. da C.; Costa, T. N. da; Franco, F. B.; Castro, R. da C.; Ferreira, J. P. L.; Souza, M. A. da S.; Santos, J. C. P. Cinética de secagem e propriedades termodinâmicas da polpa de patauá (*Oenocarpus bataua* Mart.). Brazilian Journal Food Technology, v.22, p.1-11, 2019a. https://doi.org/10.1590/1981-6723.30518

Santos, D. da C.; Leite, D. D. de F.; Lisbôa, J. F.; Ferreira, J. P. de L.; Santos, F. S. dos; Lima, T. L. B. de; Figueirêdo, R. M. F. de; Costa, T. N. da. Modelling and thermodynamic properties of the drying of acuri slices. Brazilian Journal of Food Technology, v.22, p.1-12, 2019b. https://doi.org/10.1590/1981-6723.03118

Seraglio, K. T. S.; Schulz, M.; Nehring, P.; Della Betta, F.; Valese, A. C.; Daguer, H.; Gonzaga, L. V.; Fett, R.; Costa, A. C. O. Nutritional and bioactive potential of Myrtaceae fruits during ripening. Food Chemistry, v.239, p.649-656, 2018. https://doi.org/10.1016/j.foodchem.2017.06.118

Silva, N. L.; Crispim, J. M. S.; Vieira, R. P. Kinetic and thermodynamic analysis of anthocyanin thermal degradation in acerola (*Malpighia emarginata* D.C.) pulp. Journal of Food Processing and Preservation, v.41, p.1-8, 2016. https://doi.org/10.1111/jfpp.13053

Sousa, E. P.; Figueirêdo, R. M. F.; Gomes, J. P.; Queiroz, A. J. M.; Castro, D. S.; Lemos, D. M.; Mathematical modeling of pequi pulp drying and effective diffusivity determination. Revista Brasileira de Engenharia Agrícola e Ambiental, v.21, n.7, p. 493-498, 2017. https://doi.org/10.1590/1807-1929/agriambi.v21n7p493-498

Tan, S. L.; Sulaiman, R. Color and rehydration characteristics of natural red colorant of foam mat dried *Hibiscus sabdariffa* L. powder. International Journal of Fruit Science, v.20, p.89-105, 2019. https://doi.org/10.1080/15538362.2019.1605557

Tavares, I. M. C.; Castilhos, M. B. M.; Mauro, M. A.; Ramos, A. M.; Souza, R. T.; Gómez-Alonso, S.; Gomes, E.; Silva, R.; Hermosín-Gutiérrez, I.; Lago-Vanzela, E. BRS Violeta (BRS Rúbea × IAC 1398-21) grape juice powder produced by foam mat drying. Part I: Effect of drying temperature on phenolic compounds and antioxidant activity. Food Chemistry, v.298, p.1-11, 2019. https://doi.org/10.1016/j.foodchem.2019.124971

Touil, A.; Chemkhi, S.; Zagrouba, F. Moisture diffusivity and shrinkage of fruit and cladode of opuntia ficus-indica during infrared drying. Journal of Food Processing, v.2014, p.1-9, 2014. https://doi.org/10.1155/2014/175402

Vimercati, W. C.; Macedo, L. L.; Araújo, C. S.; Teixeira, L. J. Q.; Saraiva, S. H. Efeito da temperatura na cinética de secagem em leito de espuma e na degradação de antocianina em morango. Brazilian Journal of Food Technology, v.22, p.1-12, 2019. https://doi.org/10.1590/1981-6723.22118

Zhou, M.; Li, C.; Bi, J.; Jin, X.; Lyu, J.; Li, X. Towards understanding the enhancement of moisture diffusion during intermediate-infrared drying of peach pomace based on the glass transition theory. Innovative Food Science & Emerging Technologies, v.54, p.143-151, 2019. https://doi.org/10.1016/j.ifset.2019.04.003

Zogzas, N. P.; Maroulis, Z. B.; Marinos-Kouris, D. Moisture diffusivity data compilation in foodstuffs. Drying Technology, v.14, p.2225-2253, 1996. https://doi.org/10.1080/07373939608917205